Electronic Supplementary Material (ESI) for Energy Advances.

Supporting Information

Manganese Dissolution in alkaline medium with and without concurrent oxygen evolution in $LiMn_2O_4$

Omeshwari Bisen[¶†], *Max Baumung*[¶†], *Michael Tatzel*[‡], *Cynthia A. Volkert*[†], *Marcel Risch*[¶†]*

† Institute of Materials Physics, University of Göttingen, Friedrich-Hund-Platz 1, 37077 Göttingen, Germany.

‡ Dept. of Sedimentology & Environmental Geology, University of Göttingen, Goldschmidtstr. 3, 37077 Göttingen, Germany.

¶ Young Investigator Group Oxygen Evolution Mechanism Engineering, Helmholtz Zentrum Berlin für Materialien und Energie GmbH, Hahn-Meitner-Platz 1, 14109 Berlin, Germany.

This supporting information includes 17 figures and 8 tables.

Supporting Figures

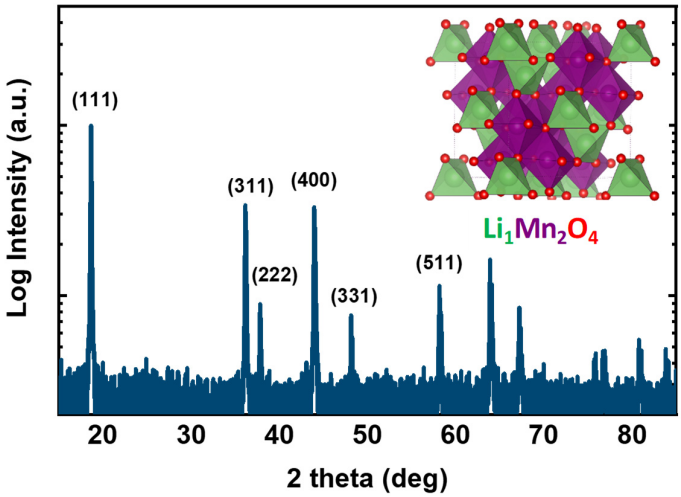

Figure S1. Indexed X-ray diffraction pattern of pristine $LiMn_2O_4$ particles (logarithmic scale). The inset shows a cubic spinel crystal structure of $LiMn_2O_4$.

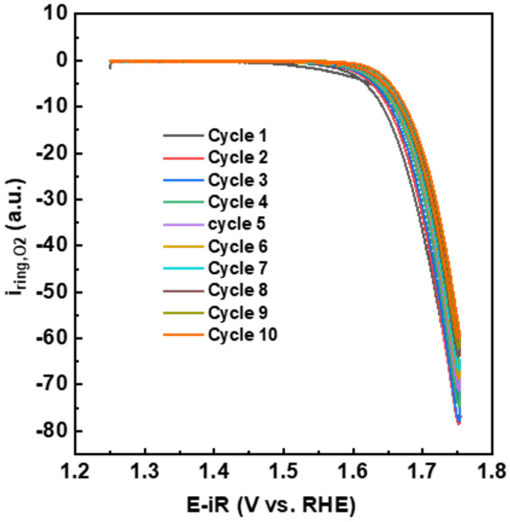

Figure S2. As-measured ring current at 0.4 V vs. RHE assigned to oxygen evolution at Pt ring (potential applied at ring is 0.4 V vs RHE) for 1st to 10th cycle.

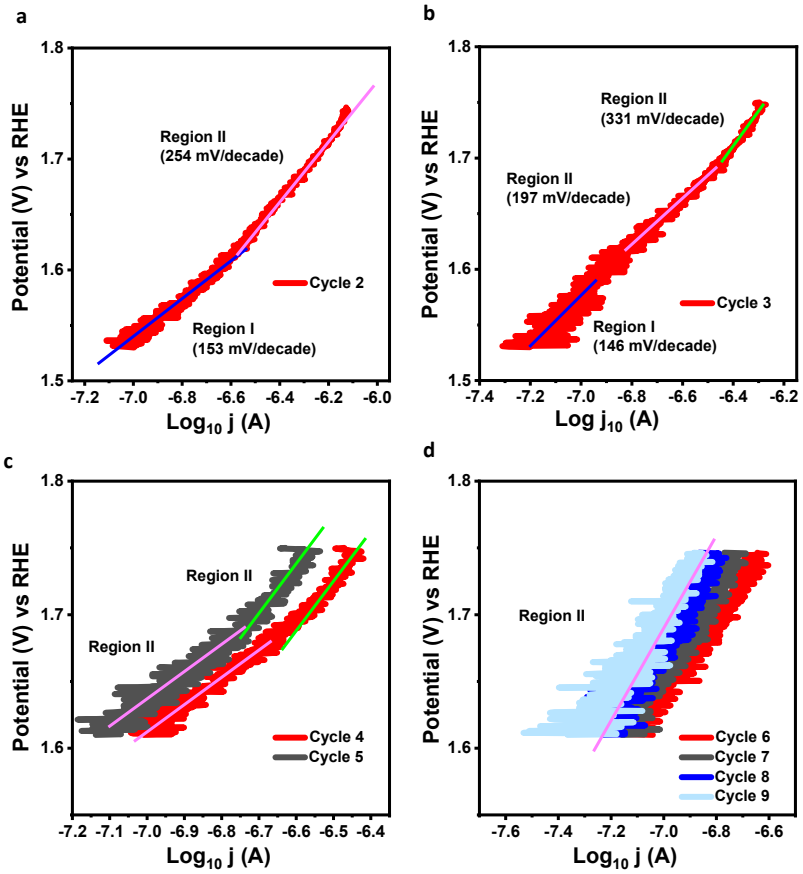

Figure S3. (a-d) Tafel slope of 2nd to 9th anodic cycle of Mn detected at a Pt ring at 1.2 V vs. RHE. Tafel slopes obtained in region I (1.4 < E < 1.6 V vs RHE) and region II (1.6 < E < 1.75 V vs RHE).

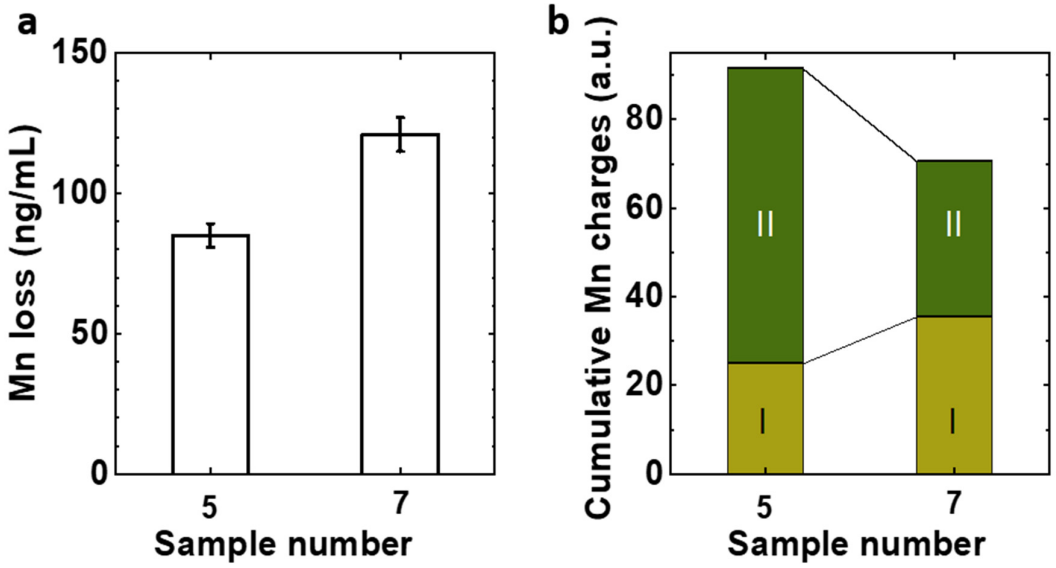

Figure S4. (a) Mn loss to electrolyte obtained from ICP-OES. Error bars indicate 5% measurement uncertainty. (b) Total Mn charges from 10 cycles corresponding to without-conditioning and conditioning + post-conditioning Mn dissolution current and different color corresponds to the distinct Mn dissolution process in region I and region II.

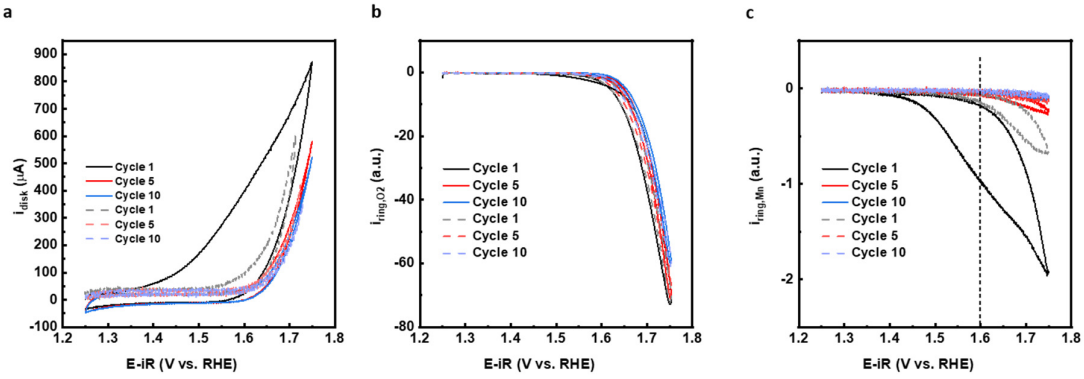

Figure S5. (a-c) CV at disk for cycle 1, 5 and 10. (b,c) CV at ring for O_2 and Mn detection for cycle 1, 5, 10, respectively. Dotted and solid lines showed the CVs with and without conditioning.

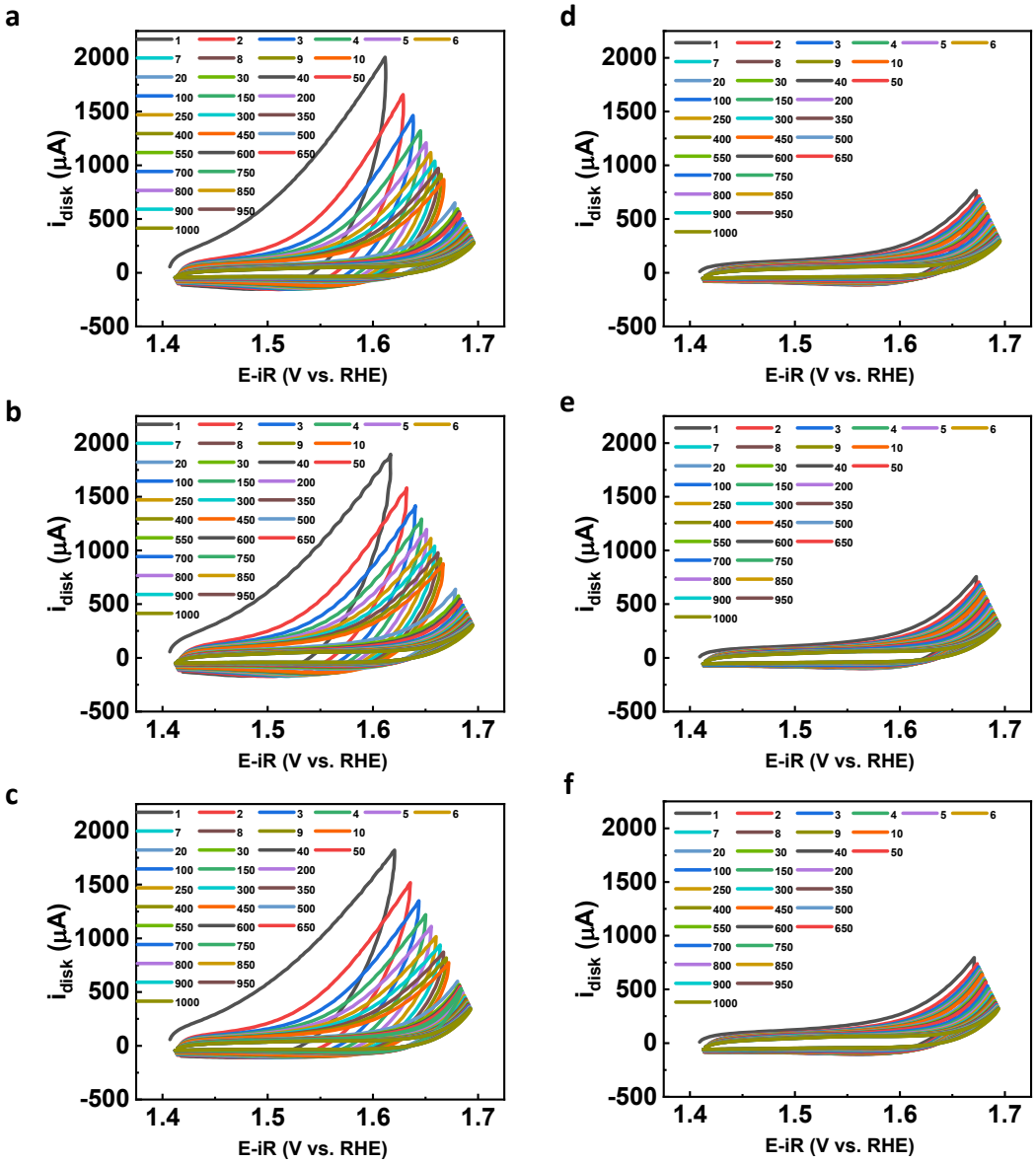

Figure S6. (a-c) Long-term tests without and (d-f) after conditioning step for 1000 cycles of $LiMn_2O_4$ with the scan rate of 100 mV/s.

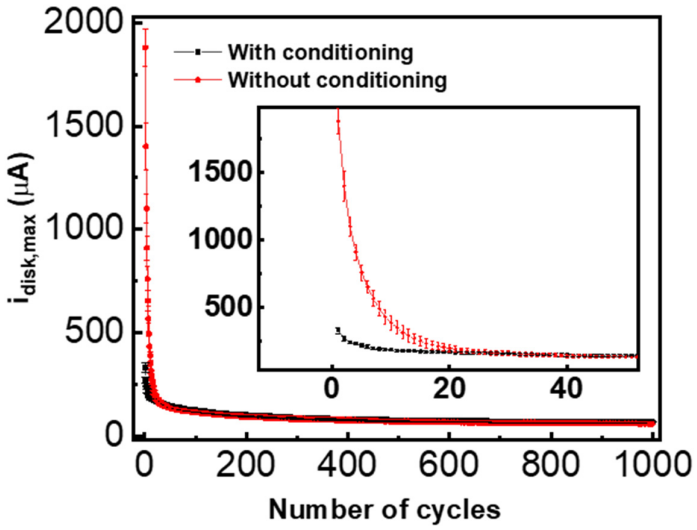

Figure S7. Change in maximal disk current density with number of cycles during long-term testing.

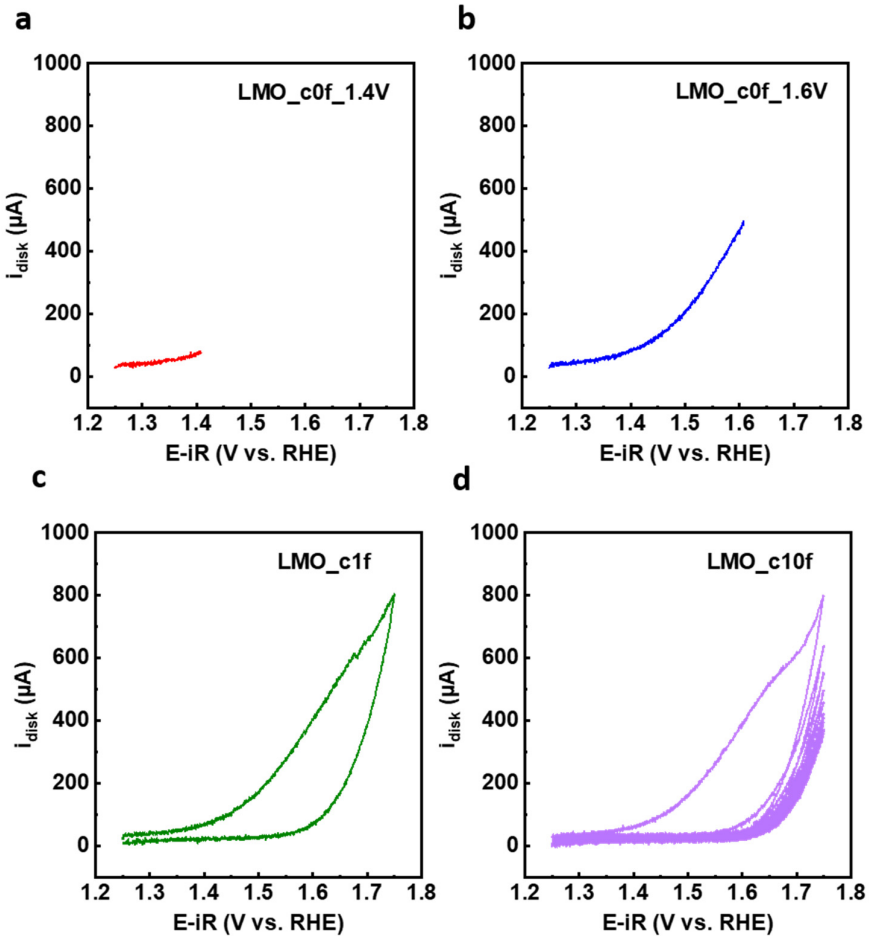

Figure S8. Electrochemical measurements for systematic XAS and XPS analysis. (1) LMO_c0f_1.4V: drop-casted particles scan up to the potential of 1.4 V vs RHE, (2) LMO_c0f_1.6 V: scans up to 1.6 V vs RHE, (3) LMO_c1f: after completion of 1 potential cycle in the potential range of 1.25-1.75 V vs RHE, (4) LMO_c10f: after 10 potential cycles in the potential range of 1.25-1.75 V vs RHE.

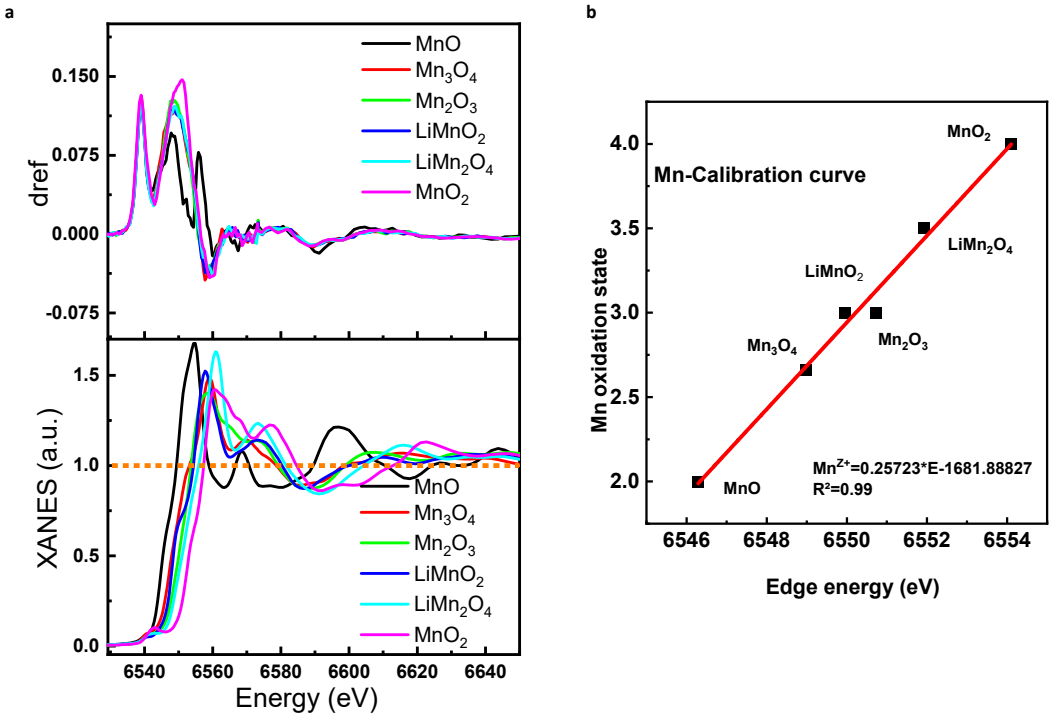

Figure S9. Mn-K edge XANES spectra and derivative of Mn reference foil collected during each XAS measurements of Mn-based reference; MnO, Mn_3O_4, Mn_2O_3, $LiMnO_2$, $LiMn_2O_4$, MnO_2. (b) Mn calibration curve obtained from nominal oxidation state of Mn-references as a function of energy of the Mn-K edge. The estimated oxidation states are shown in Table S2. The edge energy was estimated using the integral method (μ_1=1.00, μ_2=0.20). Dataset available at https://doi.org/10.5281/zenodo.10391660.

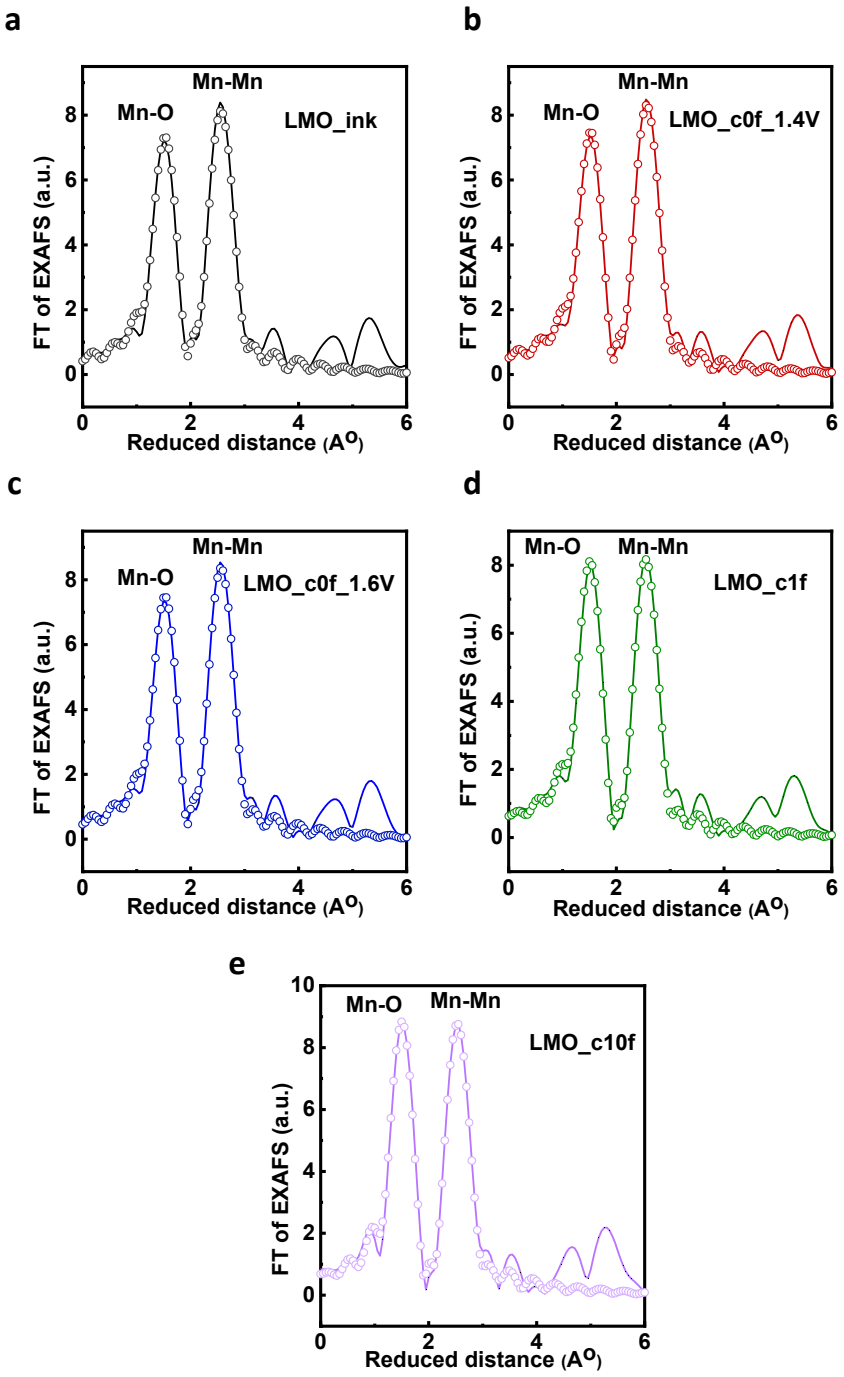

Figure S10. (a-e) FT of EXAFS spectra of LMO_ink and electrochemically processed sample LMO_c0f_1.4V, LMO_c0f_1.6V, LMO_c1f and LMO_c10f at Mn-K edge, where the solid lines represent the measurements and scattered dotted lines are respective EXAFS simulations.

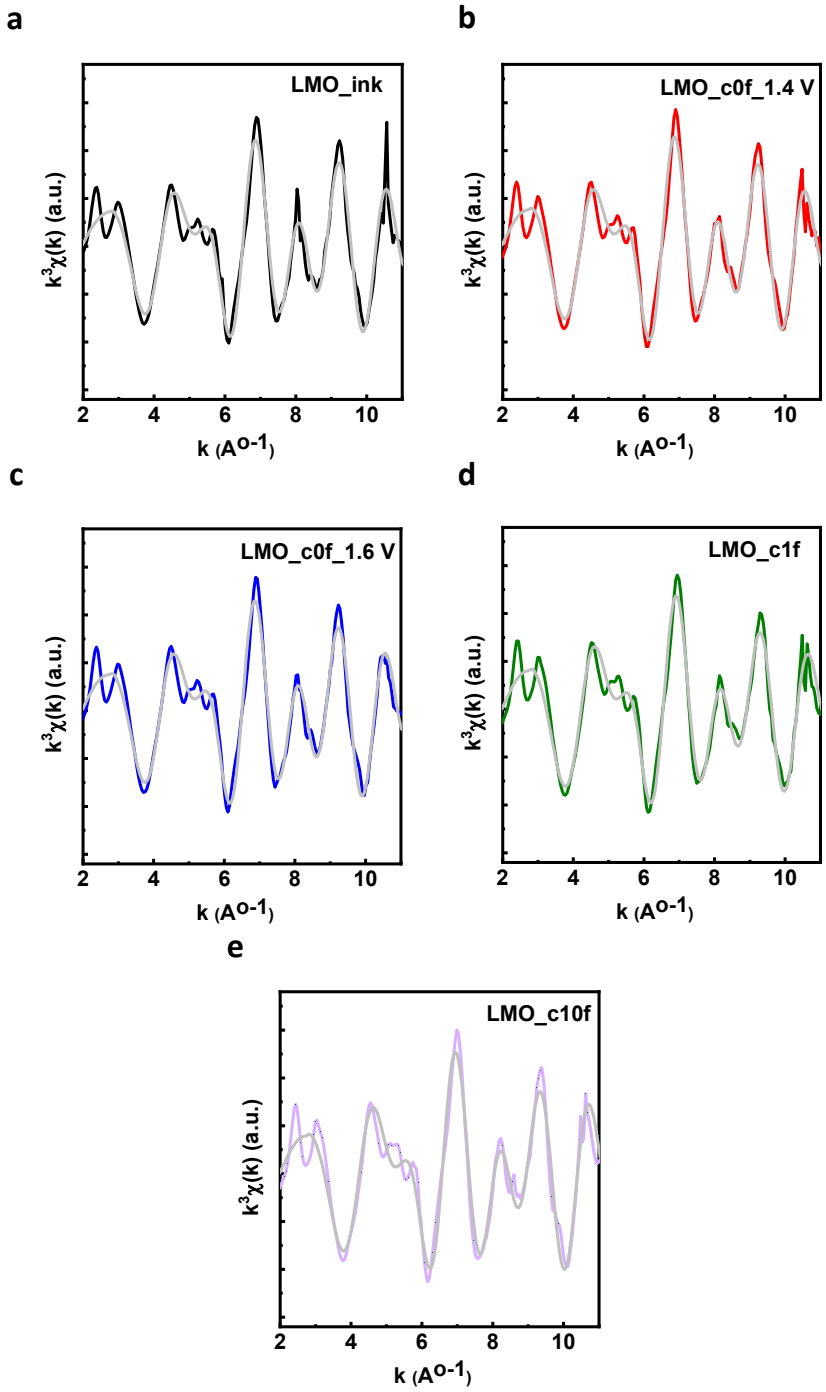

Figure S11. k^3-weighted EXAFS spectra of LMO_ink and electrochemically processed samples LMO_c0f_1.4V, LMO_c0f_1.6V, LMO_c1f and LMO_c10f recorded at the Mn-K edge. The colorful lines represent the measurements and gray lines are respective EXAFS simulations.

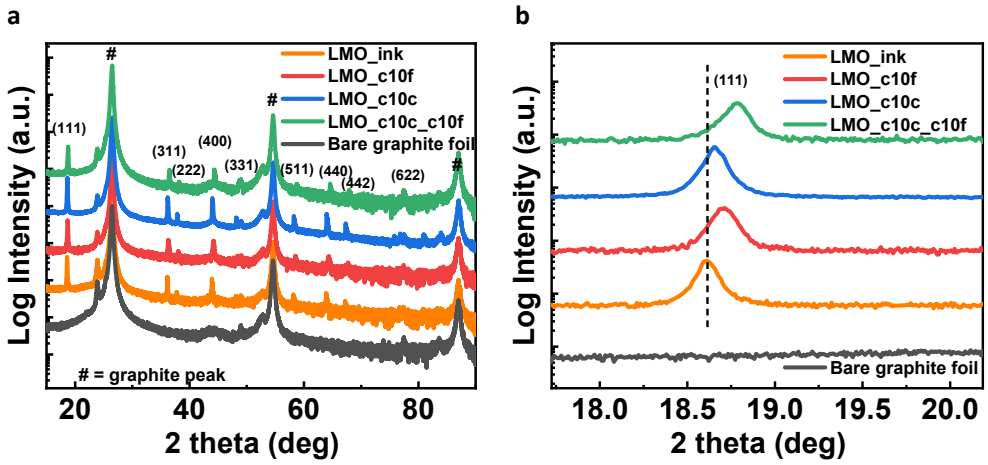

Figure S12. (a) X-ray diffraction pattern of LMO_ink, LMO_c10f, LMO_c10c and LMO_c10c_c10f and bare graphite foil as a reference. All XRD samples were drop casted on graphite foil. (b) zoomed view of (111) diffraction peak.

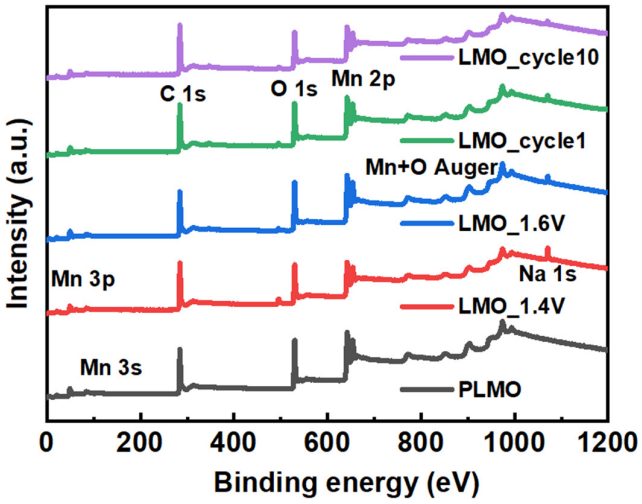

Figure S13. XPS survey scans of LMO_ink and electrochemically processed samples. All samples were drop-casted on glassy carbon disk.

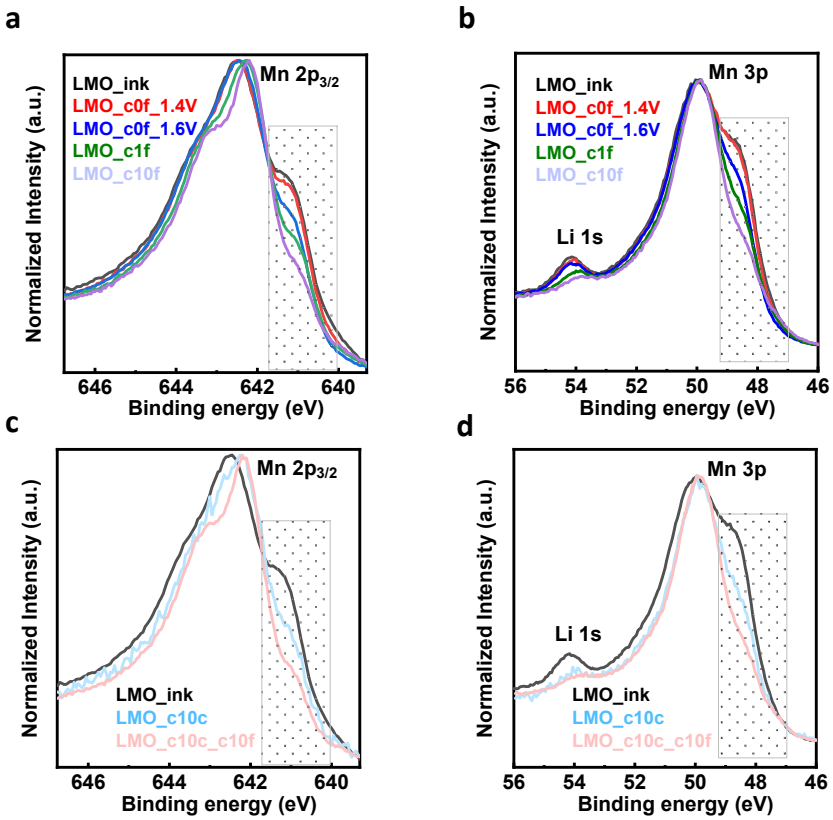

Figure S14. (a,b) Mn 2p, Mn 3p and Li 1s (shoulder at higher B.E.) HRXPS of LMO_ink, LMO_c0f_1.4V, LMO_c0f_1.6V, LMO_c1f and LMO_c10f. (c,d) Mn 2p, Mn 3p and Li 1s (shoulder at higher B.E.) HRXPS of LMO_ink, LMO_c10c and LMO_c10c_c10f.

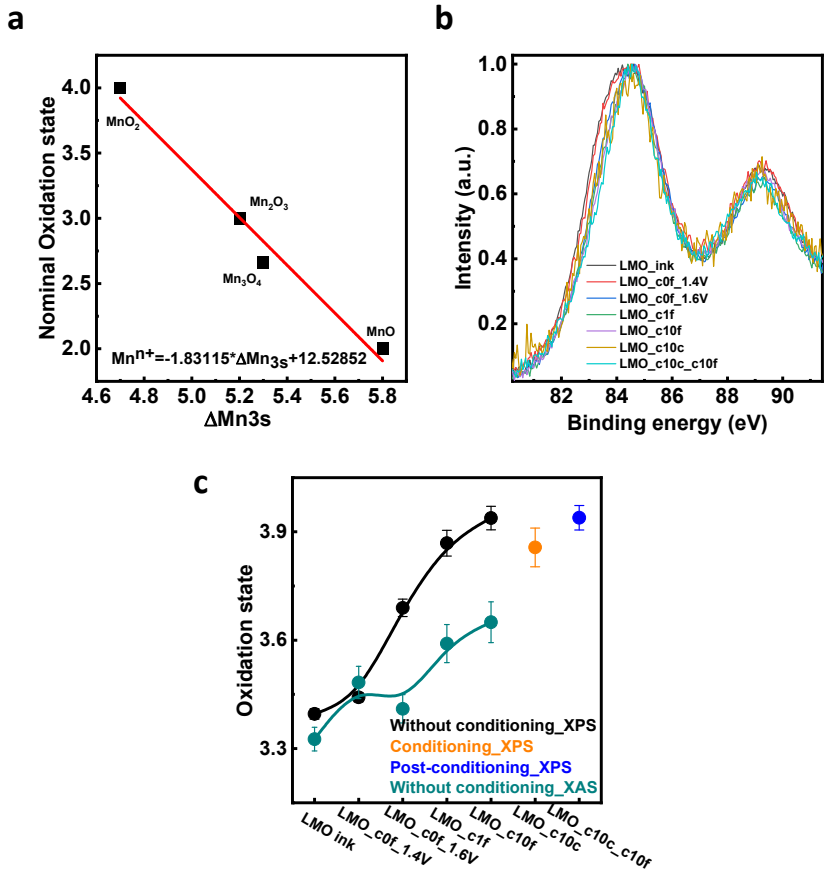

Figure S15. (a) Mn calibration curve obtained from nominal oxidation state of Mn-references (MnO (+2), Mn_3O_4 (+2.66), Mn_2O_3 (+3), MnO_2 (+4)) as a function of difference in Mn 3s multiplet splitting. (b) Mn 3s HRXPS spectra of LMO_ink and electrochemically processed samples LMO_c0f_1.4V, LMO_c0f_1.6V, LMO_c1f, LMO_c10f, LMO_c10c and LMO_c10c_c10f. (c) Bulk average oxidation state obtained from Mn-K edge XANES spectra and surface oxidation state from Mn 3s HRXPS spectra for all aforementioned samples.

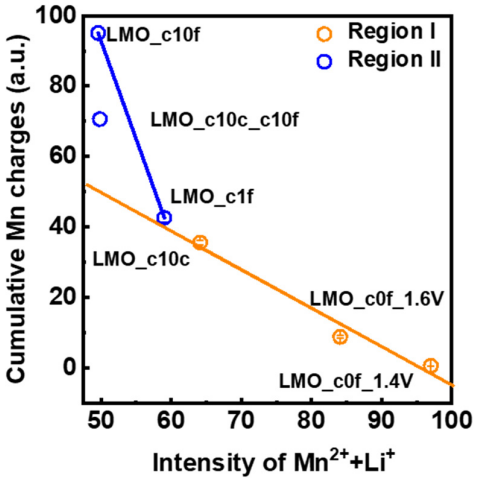

Figure S16. Correlation of cumulative Mn charges with intensity of (Mn^{2+}+Li^{+}) in Region I and Region II.

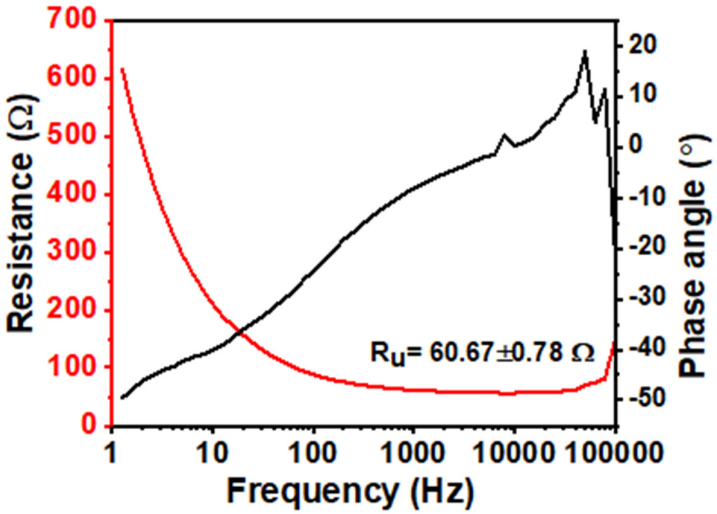

Figure S17. EIS spectra showing resistance (red) and phase angle (black) as a function of frequency collected on a $LiMn_2O_4$ decorated glassy carbon disk and uncompensated resistance was utilized for the IR correction.

Supporting Tables

Table S1. Averaged Tafel slope values for 1st to 10th anodic cycle of Mn dissolution current of LMO_ink observed at Pt ring. The values are the average of three different samples and standard deviation is reported as error.

Cycle	**Region I (1.4<E<1.6)**		**Region II (1.6<E<1.75 V vs RHE)**		**Region II (1.6<E<1.7)**		**Region II (1.7<E<1.75)**	
	Average (mV/dec)	Error (mV/dec)	Average (mV/dec)	Error (mV/dec)	Average (mV/dec)	Error (mV/dec)	Average (mV/dec)	Error (mV/dec)
1	139	4	520	44				
2	149	5	254	10				
3	146	13	229	3	198	2	331	21
4			223	1	193	2	292	33
5			231	4	194	8	255	16
6			239	6				
7			237	8				
8			253	8				
9			246	7				
10			243	1				

Table S2. Averaged Tafel slope values for 1st to 10th anodic cycle of Mn dissolution current of LMO_ink during conditioning step (in the potential window of 1.25-1.6 V vs RHE). Tafel slope were plotted in region I (1.4 < E <1.6 V vs RHE). The values are the average of three different samples and standard deviation is reported as error.

Cycle	**Region I (1.4<E<1.6)**	
	Average (mV/dec)	Error (mV/dec)
1	144	8
2	129	0.5
3	130	4
4	114	14
5	120	3
6	112	5
7	122	3
8	115	7
9	102	9
10	98	0.4

Table S3. Averaged Tafel slope values for 1st to 10th anodic cycle of Mn dissolution current of LMO_ink after conditioning step observed at Pt ring (in the potential window of 1.6-1.75 V vs RHE). The values are the average of three different samples and standard deviation is reported as error.

Cycle	**Region II (1.6<E<1.75 V vs RHE)**		**Region II (1.6<E<1.7)**		**Region II (1.7<E<1.75)**	
	Average (mV/dec)	Error (mV/dec)	Average (mV/dec)	Error (mV/dec)	Average (mV/dec)	Error (mV/dec)
1	194	16	165	13	328	26
2	205	16	171	16	257	20
3	219	16	171	11	215	25
4	209	20	162	16	202	16
5	214	27				
6	196	21				
7	189	20				
8	196	2				
9	167	17				
10	173	1				

Table S4. The Mn charge passed corresponding to Mn ring current in 1.25-1.75 V vs RHE with and without conditioning step, where conditioning step is the 10 CV in the potential window of 1.25-1.6 V vs RHE. The Mn charge has been evaluated from Figure 1b (without-conditioning), Figure 2a (during conditioning step) and Figure 2c (post-conditioning).

Cycles	**Mn charge (µF) in 1.25-1.75 V (without-conditioning)**		**Mn charge (µF) in 1.25-1.75 V (with activation step)**	
	Mn charge in 1.25-1.6 V (without-conditioning)	**Mn charge in 1.25-1.75 V (without-conditioning)**	**Mn charge in 1.25-1.6 V (during conditioning)**	**Mn charge in 1.25-1.75 V (post-conditioning)**
1	1.13E-05	4.27E-05	1.13E-05	1.16E-05
2	3.78E-06	1.53E-05	5.79E-06	5.17E-06
3	2.06E-06	8.48E-06	3.83E-06	3.55E-06
4	1.64E-06	5.96E-06	3.01E-06	2.84E-06
5	1.18E-06	4.50E-06	2.49E-06	2.51E-06
6	1.17E-06	3.75E-06	2.23E-06	2.33E-06
7	9.43E-07	3.05E-06	2.05E-06	2.08E-06
8	9.11E-07	2.76E-06	1.76E-06	1.95E-06
9	1.10E-06	2.59E-06	1.66E-06	1.73E-06
10	1.03E-06	2.42E-06	1.51E-06	1.34E-06
Total charge	**2.51E-05**	**9.15E-5**	**3.56E-5**	**3.50E-5**
			3.44E-5 + 3.75E-5 = **7.06E-5**	

Without conditioning

Charge in Region I=2.51 e-05 µF, Charge in Region II=6.64 E-05 µF

With conditioning

Charge in Region I=3.56 e-05 µF, Charge in Region II=3.50 E-05 µF

% change in charge in Region II= ((6.64 E-05 µF−3.50 E-05 µF) / 6.64 E-05 µF) *100 = ~ 47.29%

% change in total charge = ((9.15 E-05 µF−7.06 E-05 µF) / 9.15 E-05 µF) *100 = ~ 23%

Table S5. The Cumulative Mn charge passed corresponding to Mn ring current for without-conditioning, during conditioning, post-conditioning and (during conditioning + post-conditioning) experiments, where conditioning step is the 10 CV in the potential window of 1.25-1.6 V vs RHE. The Mn charge has been evaluated from Figure 1b (without-conditioning), Figure 2a (during conditioning step) and Figure 2c (post-conditioning).

	Cumulative Mn charges (µF)			
Cycles	**Without-conditioning**	**During conditioning**	**Post-conditioning**	**During conditioning + Post-conditioning**
1	4.27E-05	1.13E-05	1.16E-05	4.72E-05
2	5.80E-05	1.71E-05	1.67E-05	5.23E-05
3	6.64E-05	2.09E-05	2.03E-05	5.59E-05
4	7.24E-05	2.39E-05	2.31E-05	5.87E-05
5	7.69E-05	2.64E-05	2.56E-05	6.12E-05
6	8.06E-05	2.86E-05	2.79E-05	6.35E-05
7	8.37E-05	3.07E-05	3.00E-05	6.56E-05
8	8.65E-05	3.24E-05	3.20E-05	6.76E-05
9	8.90E-05	3.41E-05	3.37E-05	6.93E-05
10	9.15E-05	3.56E-05*	3.50E-05	7.06E-05

Cumulative Mn charges for cycle x ($1 \leq x \leq 10$) = sum of the charges of (cycle 1+ …. + cycle(x-1) + cycle x)
Cumulative Mn charges corresponding to (during conditioning + post-conditioning) for cycle x ($1 \leq x \leq 10$) = Total charges in 10 cycles during conditioning (value marked by asterisk) + cumulative charges of cycle x for post-conditioning.

Table S6. Edge energy and Mn nominal oxidation state obtained from Mn K-edge XANES spectra of LMO_ink and electrochemically processed samples. The fit equation and graph are shown in Figure S6.

Sample	**Edge energy (eV)**	**Oxidation state**
LMO_ink	6551.4	3.33 (3)
LMO_c0f_1.4V	6551.99	3.48 (4)
LMO_c0f_1.6V	6551.71	3.41 (4)
LMO_c1f	6552.47	3.60 (5)
LMO_c10f	6552.60	3.64 (6)

Table S7: EXAFS absorber-scatter averaged interatomic distance (R), co-ordination number (N) and Debye-Waller factor (σ) as determined by simulation of the k3-weighted EXAFS spectra at the Mn K edge for LMO_ink and electrochemically processed samples LMO_c0f_1.4V, LMO_c0f_1.6V, LMO_c1f and LMO_c10f. R-factor and amplitude reduction factor ($S0^2$) are also listed in table.

Sample	Parameter	Mn-O	Mn-Mn	$S0^2$	R-factor
1: LMO_ink	*N*	*6*	*6*	0.533	0.80%
	R (Å)	1.899	2.898		
	σ (Å)	0.0574	0.0589		
2: LMO_c0f_1.4V	*N*	*6*	*6*	0.575	0.54%
	R (Å)	1.898	2.896		
	σ (Å)	0.063	0.0627		
3: LMO_c0f_1.6V	*N*	*6*	*6*	0.566	0.54%
	R (Å)	1.899	2.896		
	σ (Å)	0.0614	0.061		
4: LMO_c1f	*N*	*6*	*6*	0.597	0.52%
	R (Å)	1.893	2.876		
	σ (Å)	0.0597	0.0683		
5: LMO_c10f	*N*	*6*	*6*	0.575	0.60%
	R (Å)	1.890	2.861		
	σ (Å)	0.0488	0.0625		

The number of interactions N was fixed to 6.

Table S8. ΔE_{Mn3s} and Mn surface oxidation state obtained from Mn 3s HRXPS spectra of LMO_ink and electrochemically processed samples. The fit equation and graph are shown in Figure S11.

Sample	**ΔE_{Mn3s}**	**Oxidation state**
LMO_ink	4.99	3.39 (1)
LMO_c0f_1.4V	4.96	3.44 (1)
LMO_c0f_1.6V	4.83	3.69 (2)
LMO_c1f	4.73	3.87 (3)
LMO_c10f	4.69	3.94 (3)
LMO_c10c	4.74	3.86 (5)
LMO_c10c_c10f	4.69	3.94 (3)